

## RESEARCH PAPER

# Eact, a small molecule activator of TMEM16A, activates TRPV1 and elicits pain- and itch-related behaviours

**Correspondence** Hongzhen Hu, Department of Anesthesiology, The Center for the Study of Itch, Washington University School of Medicine, St. Louis, MO 63110, USA. E-mail: huh@anest.wustl.edu

**Received** 17 April 2015; **Revised** 10 December 2015; **Accepted** 22 December 2015

Shenbin Liu<sup>1,2,\*</sup>, Jing Feng<sup>1,\*</sup>, Jialie Luo<sup>1</sup>, Pu Yang<sup>1</sup>, Thomas J Brett<sup>3</sup> and Hongzhen Hu<sup>1</sup>

<sup>1</sup>Department of Anesthesiology, The Center for the Study of Itch, Washington University School of Medicine, St. Louis, MO 63110, USA, <sup>2</sup>Department of Integrative Medicine and Neurobiology, State Key Laboratory of Medical Neurobiology, Shanghai Medical College, Fudan University, Shanghai 200032, China, and <sup>3</sup>Department of Internal Medicine, Washington University School of Medicine, St. Louis, MO 63110, USA

\*Contributed equally to this project

### BACKGROUND AND PURPOSE

TMEM16A, also known as anoctamin 1 channel, is a member of the Ca<sup>2+</sup>-activated chloride channels family and serves as a heat sensor in the primary nociceptors. Eact is a recently discovered small molecule activator of the TMEM16A channel. Here, we asked if Eact produces pain- and itch-related responses *in vivo* and investigated the cellular and molecular basis of Eact-elicited responses in dorsal root ganglia (DRG) neurons.

### EXPERIMENTAL APPROACH

We employed behavioural testing combined with pharmacological inhibition and genetic ablation approaches to identify transient receptor potential vanilloid 1 (TRPV1) as the prominent mediator for Eact-evoked itch- or pain-related responses. We investigated the effects of Eact on TRPV1 and TMEM16A channels expressed in HEK293T cells and in DRG neurons isolated from wild type and *Trpv1*<sup>-/-</sup> mice using Ca<sup>2+</sup> imaging and patch-clamp recordings. We also used site-directed mutagenesis to determine the molecular basis of Eact activation of TRPV1.

### KEY RESULTS

Administration of Eact elicited both itch- and pain-related behaviours. Unexpectedly, the Eact-elicited behavioural responses were dependent on the function of TRPV1, as shown by pharmacological inhibition and genetic ablation studies. Eact activated membrane currents and increased intracellular free Ca<sup>2+</sup> in both TRPV1-expressing HEK293T cells and isolated DRG neurons in a TRPV1-dependent manner. Eact activation of the TRPV1 channel was severely attenuated by mutations disrupting the capsaicin-binding sites.

### CONCLUSIONS AND IMPLICATIONS

Our results suggest that Eact activates primary sensory nociceptors and produces both pain and itch responses mainly through direct activation of TRPV1 channels.

### Abbreviations

DRG, dorsal root ganglia; Eact, [3,4,5-trimethoxy-*N*-(2-methoxyethyl)-*N*-(4-phenyl-2-thiazolyl)benzamide]; TG, trigeminal ganglion; WT, wild type

## Tables of Links

TARGETS	
Voltage-gated ion channels <sup>a</sup>	Other ion channels <sup>b</sup>
TRPA1	TMEM16A
TRPM8	Enzymes <sup>c</sup>
TRPV1	Collagenase 2 (MMP8)
TRPV4	Papain

LIGANDS	
Allyl isothiocyanate	Capsazepine
AMG9810	GSK1016790A
Capsaicin	Menthol

These Tables list key protein targets and ligands in this article which are hyperlinked to corresponding entries in <http://www.guidetopharmacology.org>, the common portal for data from the IUPHAR/BPS Guide to PHARMACOLOGY (Pawson *et al.*, 2014) and are permanently archived in the Concise Guide to PHARMACOLOGY 2015/16 (<sup>a,b,c</sup>Alexander *et al.*, 2015a,b,c).

## Introduction

The transmembrane protein 16 A (TMEM16A) channel, also known as anoctamin 1, is a recently identified Ca<sup>2+</sup>-activated chloride channel (CaCC) with eight transmembrane domains (Schroeder *et al.*, 2008). TMEM16A has many important physiological functions, for example, it regulates chloride secretion from exocrine glands and epithelial cells, smooth muscle contraction and pace making activity of interstitial cells of Cajal in the gut (Huang *et al.*, 2009; Iqbal *et al.*, 2012; Mroz and Keely, 2012; Singh *et al.*, 2014). TMEM16A also regulates the excitability of many types of neurons, including neurons in the spiral ganglion (Zhang *et al.*, 2015), trigeminal ganglion (TG) (Kanazawa and Matsumoto, 2014) and dorsal root ganglion (DRG) (Cho *et al.*, 2012), in which TMEM16A serves as a molecular sensor detecting noxious thermal stimuli.

Given the importance of TMEM16A in numerous physiological and pathological conditions, much attention has recently been devoted to the development of pharmacological agents with either agonistic or antagonistic action on TMEM16A. Identification of selective TMEM16A activators is not only critical to dissecting the physiological function of TMEM16A in native tissues and studying biophysical properties of TMEM16A, but also potentially for providing a novel therapeutic intervention for cystic fibrosis and other related diseases by stimulating TMEM16A-mediated chloride secretion. Eact is one of the small molecule TMEM16A activators that was discovered by a cell-based high throughput screening of  $\approx 110\,000$  compounds (Namkung *et al.*, 2011). Consistent with it being a potent TMEM16A activator, Eact directly opens TMEM16A without increasing intracellular Ca<sup>2+</sup> ([Ca<sup>2+</sup>]<sub>i</sub>), and stimulates chloride secretion from human airway epithelial cells and submucosal gland (Namkung *et al.*, 2011). Eact also causes contraction in mouse intestinal strips, activates chloride current in rat arterial myocytes (Burriss *et al.*, 2015) and inhibits oestradiol production in cultured mouse granulosa cells (Sun *et al.*, 2014).

The transient receptor potential vanilloid 1 (TRPV1) channel is a major marker of nociceptive primary sensory neurons in the DRG, TG and vagal sensory ganglia (Ahern, 2003; Caterina *et al.*, 1999; Lukacs *et al.*, 2013). TRPV1 is activated by noxious heat, tissue acidosis, endogenous ligands such as anandamide and numerous exogenous compounds including capsaicin (Ross, 2003; Tominaga *et al.*, 1998;

Watanabe *et al.*, 2003). TRPV1 also plays a crucial role in the development and maintenance of thermal hyperalgesia elicited by tissue inflammation or nerve injury (Caterina *et al.*, 2000; Davis *et al.*, 2000). More recently, TRPV1 was shown to mediate the histamine-dependent scratching response (Imamachi *et al.*, 2009).

Interestingly, both TMEM16A and TRPV1 are not only involved in detecting thermal pain, but are also highly colocalized in a subset of small-diameter DRG neurons (Cho *et al.*, 2012), suggesting the potential for functional coupling between these two channels. Therefore, pharmacological activation or inhibition of TMEM16A might affect the functions of TRPV1-expressing neurons. Moreover, in the present study, we found that Eact unexpectedly activated TRPV1 channels through a direct interaction with the capsaicin binding site. *In vivo*, Eact was found to produce both itch- and pain-related behaviours in a TRPV1-dependent manner.

## Methods

### Animals

Animal studies are reported in compliance with the ARRIVE guidelines (Kilkenny *et al.*, 2010; McGrath and Lilley, 2015). Both wild type (WT) and congenic *Trpv1*<sup>-/-</sup> mice on the C57BL/6J background were obtained from Jackson Laboratories. All mice were housed under a 12 h light/dark cycle with food and water provided *ad libitum*. All experiments were performed in accordance with the guidelines of the National Institutes of Health and the International Association for the Study of Pain, and were approved by the Animal Studies Committee at Washington University School of Medicine.

### HEK293T cell culture and transfection

HEK293T cells were grown as a monolayer using passage numbers less than 30 and maintained in DMEM (Life Technologies, Carlsbad, CA, USA), supplemented with 10% FBS (Life Technologies), 100 U mL<sup>-1</sup> penicillin, and 100  $\mu$ g mL<sup>-1</sup> streptomycin in a humidified incubator at 37°C with 5% CO<sub>2</sub>. The cells were transiently transfected with a cDNA for mouse TRPV1 (mTRPV1), individual mTRPV1 mutants, human TRPA1 (hTRPA1), hTRPM8, rat TRPV4 (rTRPV4) or mTMEM16A using Lipofectamine 2000 (Invitrogen, Carlsbad, CA, USA) with a ratio of 0.8:2. Following transfection,

the cells were maintained in DMEM at 37°C for 24 h before use. All TRPV1 mutants were made using the QuikChange II XL Mutagenesis Kit (Agilent Technologies Inc. Santa Clara, CA, USA) according to the manufacturer's directions. All mutations were confirmed by DNA sequencing.

### *siRNA knockdown of TMEM16A*

HEK293T cells plated in 48-well plates were transfected with either 200 nM TMEM16A siRNA (HSS123904; 5'-AAG UUA GUG AGG UAG GCU GGG AAC C-3', Life Technologies) or 200 nM scrambled siRNA control (12935300; 5'-GGU UCC CAG CCU ACC UCA CUA ACU U-3', Life Technologies) using Lipofectamine 2000 (Life Technologies) at a 20:2 ratio (pmol siRNA:  $\mu$ L Lipofectamine 2000); mTRPV1 was co-transfected with siRNA or scrambled siRNA control; 48 h later, cells were plated onto round coverslips and incubated for an additional 24 h. Knockdown of TMEM16A expression was assayed by Western blot.

### *Western blot*

HEK293T cells were pelleted, lysed with cell lysis buffer (25 mM Tris-HCl, pH 7.6, 150 mM NaCl, 0.1% SDS, 1 mM each, PMSE, NaF, NaVO<sub>3</sub>, 1  $\mu$ g mL<sup>-1</sup> each, leupeptin, pepstatin, aprotinin), followed by centrifugation at 12 000 *g* for 20 min. The protein concentration of the supernatant was determined by BCA Protein Assay Kit (Pierce, Rockford, IL, USA); 120  $\mu$ g protein was boiled for 3 min at 100°C with an appropriate volume of 5 $\times$  SDS-PAGE sample loading buffer (250 mM Tris-HCl, pH 6.8, 5% 2-mercaptoethanol, 10% SDS, 0.5% bromophenol blue, 50% glycerol). Samples were loaded into each lane of a 12% SDS-PAGE gel. The membrane was blocked by 5% BSA in TBS-T (50 mM Tris-HCl, pH 7.6, 140 mM NaCl, 0.1% Tween 20) at 4°C overnight and then incubated with primary and secondary antibodies diluted in blocking solution at room temperature for 3 h. Blots were developed in ECL (Pierce, Rockford, IL, USA) solution for 3 min and exposed onto a Kodak X-OMAT AR film (Eastman Kodak, Rochester, NY, USA) for 3 min. The antibodies used were rabbit anti-TMEM16A (ab84115) (1:1000, Abcam, Cambridge, MA, USA), HRP-anti-rabbit secondary antibody (1:1000, Santa Cruz, CA, USA). Mouse HRP-anti- $\beta$ -actin (1:5000, Santa Cruz, CA, USA) was used as a loading control. Densitometry analysis of TMEM16A bands and  $\beta$ -actin bands were performed using Image J software (GeneGnome, Syngene, Frederick, MD, USA). The same size square was drawn around each band to measure the density after the background near that band was subtracted. TMEM16A levels were normalized against  $\beta$ -actin levels and expressed as fold increase.

### *Isolation and short-term culture of mouse DRG neurons*

Animals were anaesthetized with isoflurane followed by cervical dislocation. The spinal column was removed and placed in ice-cold HBSS; laminectomies were performed to dissect out bilateral DRG. Neurons were acutely dissociated and maintained as described previously (Yin *et al.*, 2013, 2014). In brief, after removal of connective tissues, DRG were transferred to 1 mL Ca<sup>2+</sup>/Mg<sup>2+</sup>-free HBSS containing 2  $\mu$ L saturated NaHCO<sub>3</sub>, 0.35 mg L-cysteine, and 20 U papain (Worthington) and incubated at 37°C for 10 min. DRGs were spun down, the

supernatant was removed and 1 mL Ca<sup>2+</sup>/Mg<sup>2+</sup>-free HBSS containing 4 mg collagenase type II and 1.25 mg dispase type II (all from Sigma-Aldrich) was added and incubated at 37°C for another 10 min. After digestion, neurons were pelleted, suspended in the neurobasal medium containing 2% B-27 supplement, 1% L-glutamine, 100 U mL<sup>-1</sup> penicillin plus 100  $\mu$ g mL<sup>-1</sup> streptomycin, and 50 ng mL<sup>-1</sup> nerve growth factor, plated on a 12 mm coverslip coated with poly-L-lysine (10  $\mu$ g mL<sup>-1</sup>) and cultured under a humidified atmosphere of 5% CO<sub>2</sub>/95% air at 37°C for 18–24 h before use.

### *Live cell Ca<sup>2+</sup> imaging*

Cultured DRG neurons and HEK293T cells expressing TRP channels were loaded with 4  $\mu$ M Fura-2 AM (Life Technologies) in the culture medium at 37°C for 60 min. Cells were then washed three times and incubated in HBSS at room temperature for 30 min before use. Fluorescence at 340 and 380 nm excitation wavelengths was recorded on an inverted Nikon Ti-E microscope equipped with 340, 360 and 380 nm excitation filter wheels using NIS-elements imaging software (Nikon Instruments Inc., Melville, NY, USA). Fura-2 ratios (F340/F380) reflect changes in [Ca<sup>2+</sup>]<sub>i</sub> upon stimulation. Values were obtained from 100 to 250 cells in time-lapse images from each coverslip. Threshold of activation was defined as 3 SDs above the average (~20% above the baseline).

### *Patch-clamp recordings*

Whole-cell and single-channel patch-clamp recordings were performed using an Axon 700B amplifier (Molecular Devices, Sunnyvale, CA, USA) at room temperature (22–24°C) on the stage of an inverted phase-contrast microscope equipped with a filter set for GFP visualization. Pipettes pulled from borosilicate glass (BF 150-86-10; Sutter Instrument, Novato, CA, USA) with a Sutter P-1000 pipette puller had resistances of 2–4 and 8–10 M $\Omega$  for whole-cell and single-channel recordings, respectively, when filled with pipette solution containing 140 mM CsCl, 2 mM EGTA and 10 mM HEPES with pH 7.3 and 315 mOsm L<sup>-1</sup> osmolarity. Symmetrical solutions with the same components as that in the pipette solution were used for single-channel recordings. The Cl<sup>-</sup> free pipette solution contained 140 mM caesium acetate, 2 mM EGTA and 10 mM HEPES with pH 7.3 and 315 mOsm L<sup>-1</sup> osmolarity. A Ca<sup>2+</sup>-free extracellular solution was used for whole-cell recording to avoid Ca<sup>2+</sup>-dependent desensitization of TRPV1; this solution contained 140 mM NaCl, 5 mM KCl, 0.5 mM EGTA, 1 mM MgCl<sub>2</sub>, 10 mM glucose and 10 mM HEPES (pH was adjusted to 7.4 with NaOH, and the osmolarity was adjusted to  $\approx$ 340 mOsm L<sup>-1</sup> with sucrose). The whole-cell membrane currents were recorded using voltage ramps from -100 to +100 mV for 500 ms at a holding potential of 0 mV. Data were acquired using CLAMPPEX 10.4 software (Molecular Devices). Currents were filtered at 2 kHz and digitized at 10 kHz. Data were analysed and plotted using Clampfit 10 (Molecular Devices). Single-channel events were identified on the basis of the half-amplitude threshold-crossing criteria. Open probability was determined from idealized traces as the ratio of the sum of all open durations to the total trace duration using Clampfit 10.

### Nocifensive response

Intraplantar injection of Eact was used to induce nociceptive responses as described previously (Caterina *et al.*, 2000). Immediately after injection, mice were placed inside a Plexiglas chamber. Total time spent licking and lifting the injected hind paw was measured from video recordings (5 min). AMG9810 was administered i.p. 30 min before intraplantar injection of Eact. Control mice were injected with an equal volume of the vehicle (0.9% saline +1% DMSO +0.1% Tween 80).

### Thermal pain test

Paw withdrawal latencies in response to radiant heat were measured using the Hargreaves apparatus (IITC Life Science Inc) (Caterina *et al.*, 2000). Briefly, each mouse was placed individually in a clear Plexiglas chamber (8 × 8 × 12 cm) and acclimatized to it for at least 1 h before testing. Right hind paws of mice were injected intraplantarly with 20 µL vehicle (0.9% saline +1% DMSO +0.1% Tween 80) with or without chemicals. For assessment of thermal nociception, right hind paw withdrawal latencies were measured before (0 min) and 15, 30, 60, 90 and 120 min after injections. The infrared intensity was adjusted to obtain basal paw withdrawal latencies of 10 to 15 s. An automatic 20 s cut-off was used to prevent tissue damage.

### Scratching behaviour

Mouse scratching responses were measured as described previously (Sun and Chen, 2007; Sun *et al.*, 2009). Briefly, mice were placed individually in transparent cages for at least 30 min before assays and received Eact or vehicle control by i.d. injections into the rostral back. The number of hind limb scratching bouts directed to the injection site over a 30 min period was calculated.

All mice were randomized to experimental groups. All behavioural tests were videotaped from a side angle, and behavioural assessments were carried out by observers blind to the treatments or genotypes of the animals.

### Statistics

The data and statistical analysis comply with the recommendations on experimental design and analysis in pharmacology (Curtis *et al.*, 2015).

The concentration-response curve of Eact-activated outward currents at +60 mV was fitted with the logistic equation:  $Y = Y_{\min} + (Y_{\max} - Y_{\min}) / (1 + 10^{[(\log EC_{50} - X) \times \text{Hill slope}])}$ , where  $Y$  is the response at a given concentration,  $Y_{\max}$  and  $Y_{\min}$  are the maximum and minimum responses,  $X$  is the logarithmic value of the concentration and Hill slope is the slope factor of the curve.  $EC_{50}$  is the concentration that gives a response halfway between  $Y_{\max}$  and  $Y_{\min}$ . All data are presented as mean ± SEM for  $n$  independent observations. Student's  $t$ -test was used to analyse statistical significance between two groups. ANOVA and repeated measures tests were used to test hypotheses about effects in multiple groups occurring over time.  $P < 0.05$  was considered significantly different.

### Chemicals

Capsaicin, GSK1016790A, AMG9810 and T16Ainh-A01 were purchased from Sigma-Aldrich (St. Louis, MO, USA); Eact was from Tocris (Ellisville, MO, USA); allyl isothiocyanate was from ACROS (Geel, Belgium); menthol was from MP Biomedicals (Santa Ana, CA, USA); papain and collagenase (type 2) were from Worthington (Lakewood, NJ, USA).

## Results

### *Eact elicits both itch- and pain-related behaviours in a TRPV1-dependent manner*

TMEM16A is activated by increased intracellular free  $Ca^{2+}$  ( $[Ca^{2+}]_i$ ) evoked by activation of many GPCRs including the histamine  $H_1$  receptor and endothelin ETA receptor, which are important itch mediators (Cho *et al.*, 2012; Luo *et al.*, 2015; Yang *et al.*, 2008). Furthermore, TMEM16A is also reported to mediate the bradykinin-induced nocifensive response and is required for generating nociceptive behaviours in mouse models of thermal pain (Jin *et al.*, 2013; Liu *et al.*, 2010). We therefore asked if the TMEM16A activator Eact could also evoke itch- and pain-related behaviours *in vivo*. Indeed, i.d. injection of Eact into the rostral back of mice produced an intense scratching response (Figure 1A). Moreover, injection of Eact into hind paws of mice immediately elicited a nocifensive response, suggesting that Eact produces both acute pain and itch sensations (Figure 1B). Furthermore, paw injection of Eact evoked a robust and sustained thermal hypersensitivity lasting for at least 60 min (Figure 1C). Surprisingly, when Eact was co-applied with a selective TMEM16A inhibitor T16Ainh-A01 (A01) (Davis *et al.*, 2013), the Eact-elicited itch-related and pain-related behaviours were only partially reversed (Supporting Information Fig. S1), suggesting the existence of TMEM16A-independent targets for Eact.

The Eact-induced itch- and pain-related behaviours are reminiscent of the TRPV1-mediated histamine-dependent itch, capsaicin-induced nocifensive response and thermal hyperalgesia under inflammatory conditions. We thus speculated that TRPV1 might be involved in Eact-induced sensory hypersensitivity. To address this possibility, we used a selective TRPV1 antagonist, AMG9810, which substantially inhibits capsaicin-induced nocifensive response and Freund's complete adjuvant-induced thermal hyperalgesia (Gavva *et al.*, 2005; Ro *et al.*, 2009). When AMG9810 (50 mg  $kg^{-1}$ , i.p. injection) was applied 30 min before Eact administration, it severely attenuated Eact-induced scratching, nocifensive response and thermal hypersensitivity (Figure 1). Even more surprisingly, genetic ablation of the TRPV1 function completely abolished Eact-elicited pain-related and itch-related behaviours, suggesting that TRPV1 might be the prominent receptor for Eact-induced sensory hypersensitivity *in vivo* (Figure 1).

### *Eact activates recombinant TRPV1 channels expressed in heterologous cells*

There are a few possibilities for the involvement of TRPV1 in Eact-elicited sensory hypersensitivity, for instance, TRPV1

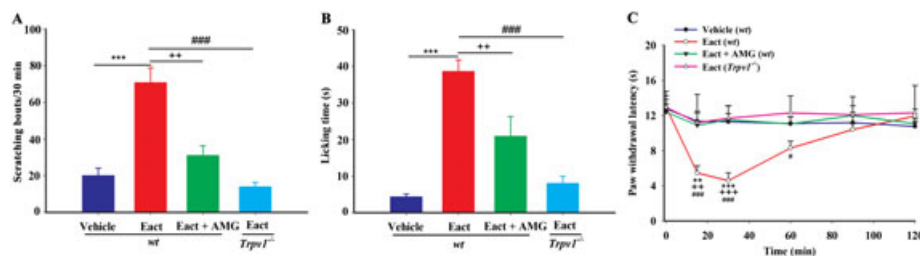


**Figure 1**

Genetic ablation or pharmacological blockade of TRPV1 function severely attenuates or abolishes Eact-induced itch- and pain-related behaviours. (A) I.d. injection of 50  $\mu\text{L}$  Eact (4.67 mM) into the rostral back induced a scratching response that was attenuated by pretreatment with AMG9810 (50 mg  $\text{kg}^{-1}$ , i.p.) and was completely absent in the *Trpv1*<sup>-/-</sup> mice. (B) Intraplantar injection of 20  $\mu\text{L}$  of Eact (4.67 mM) produced flinching and licking behaviours that were significantly reduced by i.p. injection of AMG9810 (50 mg  $\text{kg}^{-1}$ ) 30 min before paw injection of Eact. Genetic ablation of TRPV1 function abolished the nocifensive responses evoked by Eact. (C) Time course of thermal hypersensitivity in animals treated with Eact. Intraplantar injection of 20  $\mu\text{L}$  of Eact (4.67 mM) induced thermal hypersensitivity in wt mice. AMG9810 (50 mg  $\text{kg}^{-1}$ ; i.p.) significantly inhibited the effect of Eact, and Eact-elicited thermal hypersensitivity was absent in the *Trpv1*<sup>-/-</sup> mice. \*\* $P < 0.01$ , \*\*\* $P < 0.001$  Eact WT group compared with vehicle WT group; ++ $P < 0.01$ , +++ $P < 0.001$  Eact + AMG WT group compared with Eact WT group; # $P < 0.05$ , ### $P < 0.001$  Eact *Trpv1*<sup>-/-</sup> group compared with Eact WT group;  $n = 7\text{--}8$  mice per group. AMG = AMG9810.

could act as a mediator of the TMEM16A signalling complex as recent studies showed that TMEM16A functionally interacts with TRP channels including TRPV1 and TRPV4 (Takayama *et al.*, 2014; Takayama *et al.*, 2015), and we also found that co-expression of TMEM16A with TRPV1 could enhance capsaicin-activated currents in HEK293T cells (Supporting Information Fig. S2). The other possibility is that Eact could directly activate TRPV1. We tested this possibility in mTRPV1-expressing HEK293T cells using live cell  $\text{Ca}^{2+}$  imaging and whole-cell patch-clamp recordings. Indeed, Eact (at 100  $\mu\text{M}$ ) evoked a substantial increase in  $[\text{Ca}^{2+}]_i$  in cells expressing mTRPV1, which were also activated by the selective TRPV1 agonist capsaicin (500 nM) (Figure 2A). In marked contrast, Eact had no effect on HEK293 cells transiently transfected with other thermally activated TRP channels (ThermoTRPs) including human TRPA1, human TRPM8 and rat TRPV4, suggesting that Eact selectively activates TRPV1 among the ThermoTRPs tested.

Consistent with the results from the  $\text{Ca}^{2+}$  imaging studies, Eact also activated membrane currents in mTRPV1-expressing HEK293T cells in a concentration-dependent manner with an  $\text{EC}_{50}$  of  $11.6 \pm 2.5$   $\mu\text{M}$  (Figure 2B–D). The current traces in response to a voltage ramp ( $-100$  to  $+100$  mV) for Eact were similar to that activated by capsaicin or camphor (Figure 2B and C) (Caterina *et al.*, 1997; Xu *et al.*, 2005). Although HEK293T cells express endogenous TMEM16A (Sala-Rabanal *et al.*, 2015), knockdown of TMEM16A by small interference RNA (siRNA) did not affect Eact activation of mTRPV1 in HEK293T cells (Supporting Information Fig. S3), suggesting that activation of TRPV1 by Eact does not require endogenously expressed TMEM16A in the HEK293T cells. The maximal response evoked by 100  $\mu\text{M}$  Eact was  $69.4 \pm 0.9\%$  of the response evoked by 3  $\mu\text{M}$  capsaicin (the current density of 100  $\mu\text{M}$  Eact was  $404.0 \pm 24.4$  pA  $\text{pF}^{-1}$ , compared with  $581.8 \pm 33.9$  pA  $\text{pF}^{-1}$  by 3  $\mu\text{M}$  capsaicin) (Figure 2D), indicating Eact has a lower efficacy than capsaicin to activate TRPV1. Furthermore, Eact increased single-channel activities in inside-out patches excised from the TRPV1-expressing HEK293T cells (Figure 2E), suggesting that Eact directly activates recombinant TRPV1 in the absence of intracellular signalling molecules.

### Molecular basis of Eact activation of TRPV1

The TRPV1 channel is an allosterically regulated modular protein and activators like capsaicin, protons and noxious temperature stimuli activate TRPV1 through distinct protein domains (Aneiros *et al.*, 2011). To investigate the amino acid residues involved in Eact activation of TRPV1, we made TRPV1 mutants in which activation by temperature (N629K, N653T/N654T), proton (E601Q and E649Q) or capsaicin (R115A, Y512A, S513Y, Y512A/S513Y, M548L and T551A) was severely impaired. We obtained concentration-response curves of Eact-activated whole-cell currents and compared  $\text{EC}_{50}$  values of WT and mutant TRPV1 constructs individually transfected in HEK293T cells. We found that Eact-activated currents were severely attenuated in the S513Y, Y512A/S513Y mutants in which the Eact  $\text{EC}_{50}$  values were increased by at least sixfold when compared with WT TRPV1 (Figure 3B and Table 1). Additionally,  $\text{EC}_{50}$  values for Eact in mutants S513A, M548L and T550A were also increased, although not as high as that in the S513Y, Y512A/S513Y mutants (Figure 3B and Table 1). In contrast, TRPV1 mutants with impaired proton or heat activation had comparable Eact  $\text{EC}_{50}$  values as the WT TRPV1 (Figure 3A and Table 1). These results suggest that the domains that participated in capsaicin activation of TRPV1 are also required for the interaction between Eact and TRPV1.

### Eact activates endogenous TRPV1 expressed by DRG neurons

To further address whether Eact could activate native TRPV1 channels, we examined the effect of Eact on membrane currents and  $[\text{Ca}^{2+}]_i$  responses in dissociated mouse DRG neurons. Administration of Eact (100  $\mu\text{M}$ ) activated a large outwardly rectifying current in cultured small-diameter WT DRG neurons (Figure 4A and B). The Eact-activated current was substantially reduced by co-application of TRPV1 inhibitors AMG9810 (0.1  $\mu\text{M}$ ) and capsazepine (10  $\mu\text{M}$ ), and was absent from the *Trpv1*<sup>-/-</sup> DRG neurons (Figure 4, Supporting Information Fig. S4). Moreover, co-application of a selective TMEM16A inhibitor A01 did not significantly affect the

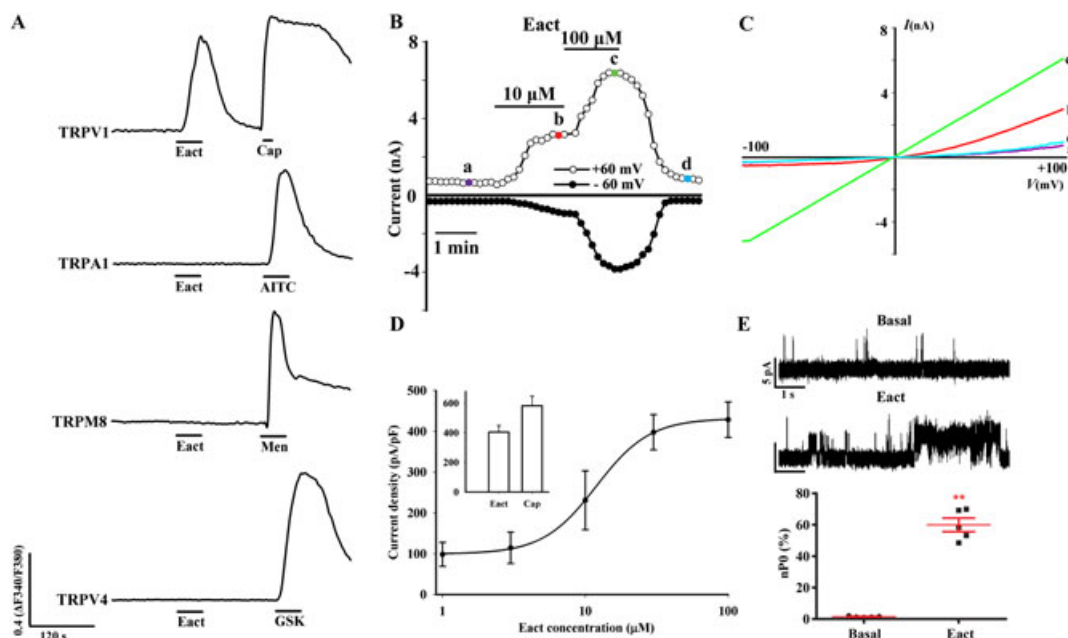


**Figure 2**

Eact activates recombinant TRPV1. (A) The representative trace on top shows that Eact (100  $\mu\text{M}$ ) evoked an increase in  $[\text{Ca}^{2+}]_i$  in a HEK293T cell transiently transfected with mTRPV1, which also responded to capsaicin (Cap: 500 nM). The second to fourth representative traces from the top illustrate that Eact (100  $\mu\text{M}$ ) had no effect on  $[\text{Ca}^{2+}]_i$  in hTRPA1-, hTRPM8- or rTRPV4-expressing HEK293T cells, which were activated by their respective agonists allyl isothiocyanate (AITC, 100  $\mu\text{M}$ ), menthol ((-)-Men, 100  $\mu\text{M}$ ) or GSK1016790A (GSK) (0.3  $\mu\text{M}$ ) respectively. (B) Representative current traces show that Eact activated an outward (at +60 mV) and an inward (at -60 mV) current in a concentration-dependent manner in a mTRPV1-expressing HEK293T cell. (C) Representative current-voltage (I-V) curves taken at the specified time points from the trace on (B) illustrate that an outwardly rectifying whole-cell current was evoked by Eact at 10  $\mu\text{M}$  (b), whereas 100  $\mu\text{M}$  (c) Eact activated a current with a linear I-V relationship in a mTRPV1-expressing HEK293T cell (a refers to the baseline response). (D) The concentration-response curve of Eact-activated outward currents at +60 mV. The inset graph illustrates the maximal current densities evoked by saturating concentrations of Eact (100  $\mu\text{M}$ ) and capsaicin (3  $\mu\text{M}$ ). (E) The single-channel current traces on top show that Eact increased single channel opening in an inside-out membrane patch isolated from a mTRPV1-expressing HEK293T cell. The graph at the bottom illustrates that Eact significantly increased single channel open probability (nPo) in inside-out patches excised from mTRPV1-expressing HEK293T cells (\*\* $P < 0.0001$  vs. baseline response).

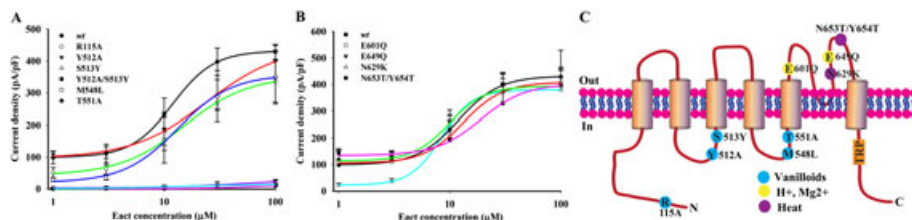


**Figure 3**

Structural requirements for Eact activation of TRPV1. (A) Concentration-response curves of Eact-activated outward currents at +60 mV in WT and TRPV1 mutants with disrupted domains for proton or heat activation of TRPV1. (B) Concentration-response curves of Eact-activated outward currents at +60 mV in WT and TRPV1 mutants carrying single or double point mutations in the 'vanilloid-binding pocket'. (C) Schematic diagram illustrates structural elements required for activation/modulation of TRPV1 channels by capsaicin, protons and heat.

Eact-activated current in WT DRG neurons (Supporting Information Fig. S5). Furthermore, the Eact-activated current persisted in WT DRG neurons recorded with a  $\text{Cl}^-$  free pipette solution (Supporting Information Fig. S6), suggesting that the Eact-activated current is not carried by chloride. These results suggest that TRPV1 is a Eact receptor in cultured DRG neurons, and activation of TRPV1 by Eact does not require TMEM16A.

Additionally, consistent with the  $\text{Ca}^{2+}$  imaging results from the mTRPV1-expressing HEK293T cells, bath application of Eact (100  $\mu\text{M}$ ) alone elicited a robust  $[\text{Ca}^{2+}]_i$  response in  $32.7 \pm 2.2\%$  of DRG neurons tested, all of which responded to capsaicin (Figure 5A and B). Interestingly, capsaicin (500 nM) increased  $[\text{Ca}^{2+}]_i$  in a larger population of DRG neurons ( $51.8 \pm 5.1\%$ ) than that activated by Eact, suggesting that not all TRPV1-expressing neurons responded to Eact

**Table 1**

EC<sub>50</sub> values and Hill coefficients of Eact-activated response in WT and TRPV1 mutants

	<i>n</i> <sub>H</sub> , Hill coefficient	EC <sub>50</sub> (μM)	<i>n</i>
WT	2.0 ± 0.4	11.6 ± 2.5	11
R115A	1.9 ± 1.1	16.2 ± 4.1	7
Y512A	1.2 ± 0.9	26.3 ± 5.1*	8
S513Y	1.2 ± 0.1	63.5 ± 17.6**	9
Y512A/S513Y	2.6 ± 1.1	67.5 ± 19.1**	9
M548I	1.0 ± 0.7	15.9 ± 2.5	6
T551A	1.4 ± 0.9	13.6 ± 4.9	7
E601Q	2.9 ± 0.6	13.6 ± 0.7	6
E649Q	2.9 ± 1.1	10.5 ± 1.3	6
N629K	3.6 ± 0.4	8.9 ± 2.7	6
N653T/Y654T	2.7 ± 0.6	19.3 ± 5.5	6

\**P* < 0.05.

\*\**P* < 0.001 versus *wt.*

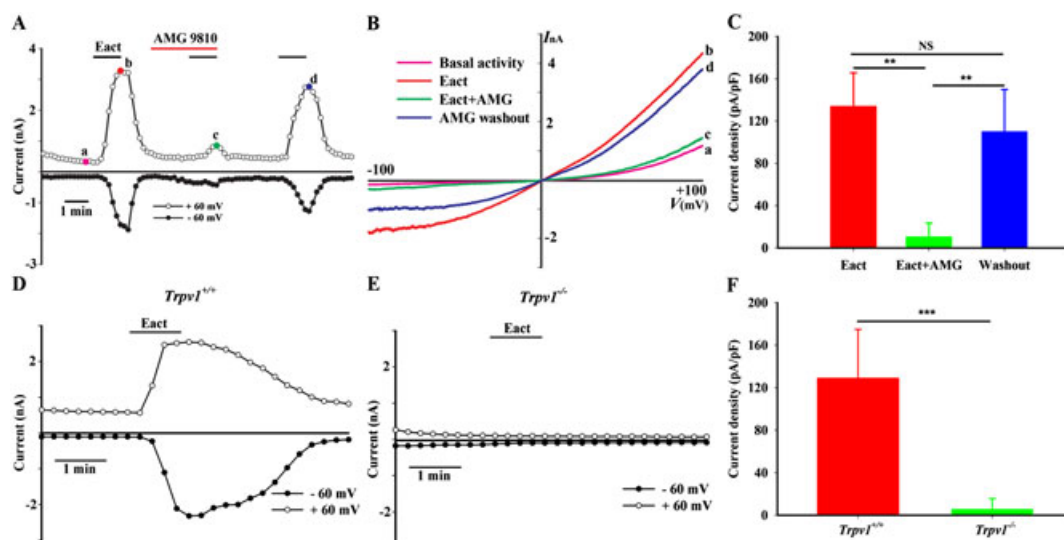
(Figure 5C). As expected, pharmacological inhibition by AMG9810 (0.1 μM) or genetic ablation of the TRPV1 function almost completely abolished the Eact-evoked [Ca<sup>2+</sup>]<sub>i</sub> responses, while allyl isothiocyanate still elicited comparable [Ca<sup>2+</sup>]<sub>i</sub> responses in both *wt.* and TRPV1-deficient DRG neurons (Figure 5B and C). Collectively, these results suggest that TRPV1 is the primary mediator of Eact-induced acute excitatory responses in the primary sensory neurons.

## Discussion

Our study provided the first evidence that Eact, a selective activator of TMEM16A, directly activates the TRPV1 channels in sensory nociceptors and produces itch, acute nociception and thermal hypersensitivity. Eact interacts with the cytosolic amino acid residues required for capsaicin activation of TRPV1. These results suggest that Eact is a potent activator of the itch- and pain-initiating TRPV1 channel, although this compound had been shown to be selective for TMEM16A.

Our data show that Eact induced a robust [Ca<sup>2+</sup>]<sub>i</sub> response in HEK293T cells transiently transfected with TRPV1, but not TRPA1, TRPM8 or TRPV4. The effect of Eact on the mTRPV1-expressing HEK293T cells was not affected by siRNA knock-down of the endogenous TMEM16A. Additionally, Eact activated single channel currents in the inside-out membrane patches isolated from the mTRPV1-expressing HEK293T cells, suggesting that this agonistic action of Eact is most likely resulting from a direct effect of the drug on TRPV1 but not through releasing intracellular second messengers. Moreover, Eact also activated membrane currents and evoked a [Ca<sup>2+</sup>]<sub>i</sub> response in DRG neurons through TRPV1 as supported by both pharmacological inhibition and genetic ablation studies.

TRPV1 is a critical molecular sensor for noxious heat and a key contributor to inflammatory thermal hyperalgesia (Caterina *et al.*, 2000; Davis *et al.*, 2000; Tominaga *et al.*, 1998). Although some studies have reported that mice lacking TRPV1 display heat avoidance behaviours, TRPV1-deficient neurons still respond to heat stimulation (Basbaum *et al.*, 2009; Woodbury *et al.*, 2004), suggesting the presence of

**Figure 4**

Pharmacological inhibition and genetic ablation of TRPV1 function inhibits Eact-activated membrane currents in DRG neurons. (A) Representative current traces show that Eact (100 μM) activated an outward current at +60 mV and an inward current at -60 mV in a WT DRG neuron. The whole-cell currents evoked by Eact were substantially suppressed by the selective TRPV1 antagonist AMG9810 (0.1 μM). The inhibitory effect of AMG9810 was partially reversible after washout. (B) Current-voltage relationship of Eact-activated current taken at the time points specified in (A). (C) Quantification of current responses to Eact in DRG neurons voltage clamped at -60 mV. AMG9810 (0.1 μM) significantly inhibited the Eact response (\*\**P* < 0.01, NS: no significant difference, *n* = 8). (D) and (E) Representative traces show that Eact (100 μM) activated an outward current at +60 mV and an inward current at -60 mV in a *Trpv1*<sup>+/+</sup> (D), but not a *Trpv1*<sup>-/-</sup> DRG neuron (E). (F) Comparison of the peak Eact current densities between *Trpv1*<sup>+/+</sup> (*n* = 9) and *Trpv1*<sup>-/-</sup> DRG neurons (*n* = 23). AMG = AMG9810.

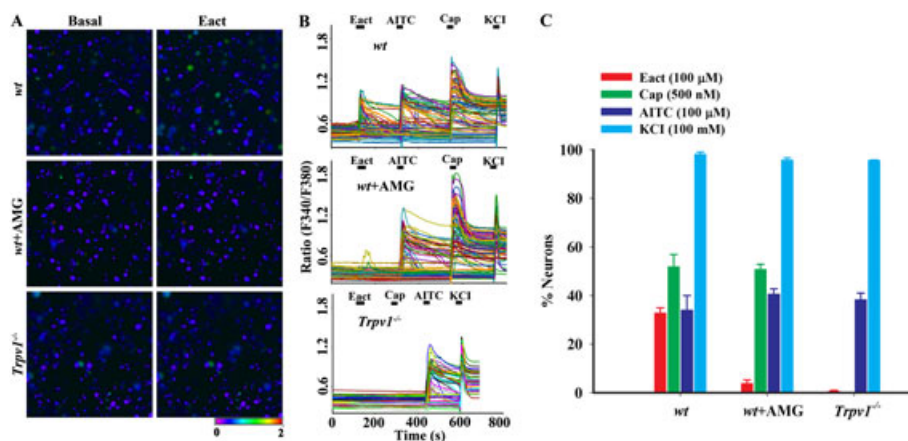


## Figure 5

Eact evokes  $[Ca^{2+}]_i$  responses in a subset of DRG neurons in a TRPV1-dependent manner. (A) Representative Fura-2 ratiometric images of cultured DRG neurons show that Eact-evoked  $[Ca^{2+}]_i$  response in a subset of DRG neurons from WT mice was significantly reduced by AMG9810 and nearly abolished by genetic ablation of the TRPV1 function. The colour of the neurons switching from blue to green or red indicates an increase in  $[Ca^{2+}]_i$ . (B) Representative traces illustrate that Eact and capsaicin elicited  $[Ca^{2+}]_i$  responses in WT but not *Trpv1*<sup>-/-</sup> DRG neurons. AMG9810 severely inhibited the Eact-induced  $[Ca^{2+}]_i$  response. AITC evoked a comparable  $[Ca^{2+}]_i$  response in both WT and *Trpv1*<sup>-/-</sup> DRG neurons. Each trace corresponds to the change in fluorescence ratio in a single neuron. Neurons were exposed to 100 μM Eact, 500 nM capsaicin, 100 μM AITC and 100 mM KCl for the indicated times. (C) Percentage of DRG neurons responding to Eact, capsaicin, AITC and KCl in neurons isolated from WT or *Trpv1*<sup>-/-</sup> mice ( $n \geq 720$  per genotype for Eact). Cap, capsaicin.

additional heat sensors. TMEM16A was recently identified as a heat-sensitive channel that was activated by temperatures greater than 44°C (Cho *et al.*, 2012). Moreover, nearly 78% of TMEM16A-immunoreactive small-diameter DRG neurons express TRPV1 (Cho *et al.*, 2012). RNAi knockdown or genetic deletion of TMEM16A from DRG neurons also substantially attenuated thermal hyperalgesia in both inflammatory and neuropathic pain models (Lee *et al.*, 2014; Liu *et al.*, 2010). Moreover, a recent study also showed that Eact activated DRG neurons and induced pain response, both of which were suppressed by the TMEM16A inhibitor A01 (Deba and Bessac, 2015). Indeed, we also found that co-expression of TMEM16A potentiated capsaicin-activated currents in mTRPV1-expressing HEK293T cells, suggesting that Eact activation of TMEM16A might also contribute to Eact-elicited sensory hypersensitivity. On the other hand, although the selective TMEM16A inhibitor A01 was able to partially suppress Eact-elicited pain- and itch-related behaviours *in vivo*, it did not significantly suppress the Eact-activated whole-cell membrane current in DRG neurons. Furthermore, we could not record the Eact-activated current in the *Trpv1*<sup>-/-</sup> DRG neurons. One explanation for our findings is that TRPV1 function is required for TMEM16A-mediated responses in the primary nociceptors. Indeed, TRPV1 and TMEM16A have been shown to interact physically and TRPV1-mediated  $Ca^{2+}$  influx subsequently activates TMEM16A (Takayama *et al.*, 2015). Moreover, TRPV4 is also found to functionally interact with TMEM16A to modulate water transport in the choroid plexus (Takayama *et al.*, 2014). Therefore, our results do not argue against the existence of functional TMEM16A in the primary sensory neurons but support the hypothesis that Eact activation of TRPV1 is an upstream event of TMEM16A activation in the same DRG neurons. Thus, although A01 could not suppress Eact activation of TRPV1, it might be able to inhibit downstream events mediated by TMEM16A.

Although different experimental settings, cell culture conditions, and differences between HEK293T cells and DRG neurons might partly account for the discrepancy of Eact responses in DRG and heterologous cells between these two studies (Deba and Bessac, 2015), our results using TRPV1 knockout mice clearly demonstrated that Eact-induced excitation and sensory hypersensitivity require functional TRPV1 channels, suggesting that Eact is not an ideal tool to dissect the function of TMEM16A in the primary sensory neurons because it could directly activate TRPV1 in the same cells. Because TRPV1 is a dominant initiator of pain and itch in the primary sensory neurons, Eact activation of TRPV1 could override TMEM16A-mediated Eact responses. Future studies using TMEM16A knockout mice will be required to provide a clear conclusion.

TRPV1 is also a critical itch receptor downstream of histamine H<sub>1</sub> receptor signalling (Imamachi *et al.*, 2009). Previous studies also showed that itch-causing substances, such as ET-1 and histamine evoked inward chloride currents in the mTMEM16A-expressing HEK293 cells (Cho *et al.*, 2012; Yang *et al.*, 2008). Furthermore, the blockers of sodium-potassium-chloride co-transporter-1, which accumulates Cl<sup>-</sup> inside of cells, reduced histamine-induced itch and flare in humans (Willis *et al.*, 2004), suggesting that TMEM16A may be critically involved in itch initiation in sensory neurons. However, although we found that i.d. injection of Eact into the rostral back could induce itch-related behaviours, these scratching responses were almost abolished by pharmacological inhibition or genetic ablation of the TRPV1 function. Although A01 also partially suppressed the Eact-elicited scratching, as discussed above, the exact role of TMEM16A in itch signalling transmission warrants further studies using the TMEM16A knockouts.

Taken together, our data indicate that the TMEM16A activator Eact activates both native and recombinant TRPV1

channels. This new finding should lead to a more careful interpretation of the effects of Eact on the excitability of neurons that are known to express TRPV1, for instance, primary nociceptors from the DRG or TG. Furthermore, the agonistic action of Eact on TRPV1 should also be taken into consideration for interpretation of the results related to TMEM16A-mediated pain- and itch-related behaviours if Eact is used as a pharmacological tool. Moreover, the sensory hypersensitivity elicited by Eact and potentially other structurally-related Ca<sup>2+</sup>-activated chloride channel activators might present an unwanted side effect for their applications to treat cystic fibrosis and related diseases.

## Acknowledgements

This work was supported partly by grants from the National Institutes of Health, R01RGM101218 and R01DK103901 (to H. H.), and R01HL119813 (to T. J. B.), The Center for the Study of Itch of Department of Anesthesiology at Washington University School of Medicine to H. H. and China Scholarship funding to S. L.

## Author contributions

S.L., J.F., J.L. and P.Y. performed the research; S.L. and H.H. designed the research; S.L. and J.F. analysed the data; S.L., T.J.B. and H.H. wrote the paper.

## Conflict of interest

The authors declare no conflicts of interest.

## Declaration of transparency and scientific rigour

This Declaration acknowledges that this paper adheres to the principles for transparent reporting and scientific rigour of pre-clinical research recommended by funding agencies, publishers and other organisations engaged with supporting research.

## References

Ahern GP (2003). Activation of TRPV1 by the satiety factor oleylethanolamide. *J Biol Chem* 278: 30 429–30 434.

Alexander SPH, Catterall WA, Kelly E, Marrion N, Peters JA, Benson HE, *et al.* (2015a). The Concise Guide to PHARMACOLOGY 2015/16: Voltage-gated ion channels. *Br J Pharmacol* 172: 5904–5941.

Alexander SPH, Peters JA, Kelly E, Marrion N, Benson HE, Faccenda E, *et al.* (2015b). The Concise Guide to PHARMACOLOGY 2015/16: Other ion channels. *Br J Pharmacol* 172: 5942–5955.

Alexander SPH, Fabbro D, Kelly E, Marrion N, Peters JA, Benson HE, *et al.* (2015c). The Concise Guide to PHARMACOLOGY 2015/16: Enzymes. *Br J Pharmacol* 172: 6024–6109.

Aneiros E, Cao L, Papakosta M, Stevens EB, Phillips S, Grimm C (2011). The biophysical and molecular basis of TRPV1 proton gating. *EMBO J* 30: 994–1002.

Basbaum AI, Bautista DM, Scherrer G, Julius D (2009). Cellular and molecular mechanisms of pain. *Cell* 139: 267–284.

Burris SK, Wang Q, Bulley S, Neeb ZP, Jaggar JH (2015). 9-Phenanthrol inhibits recombinant and arterial myocyte TMEM16A channels. *Br J Pharmacol* 172: 2459–2468.

Caterina MJ, Leffler A, Malmberg AB, Martin WJ, Trafton J, Petersen-Zeitz KR, *et al.* (2000). Impaired nociception and pain sensation in mice lacking the capsaicin receptor. *Science* 288: 306–313.

Caterina MJ, Rosen TA, Tominaga M, Brake AJ, Julius D (1999). A capsaicin-receptor homologue with a high threshold for noxious heat. *Nature* 398: 436–441.

Caterina MJ, Schumacher MA, Tominaga M, Rosen TA, Levine JD, Julius D (1997). The capsaicin receptor: a heat-activated ion channel in the pain pathway. *Nature* 389: 816–824.

Cho H, Yang YD, Lee J, Lee B, Kim T, Jang Y, *et al.* (2012). The calcium-activated chloride channel anoctamin 1 acts as a heat sensor in nociceptive neurons. *Nat Neurosci* 15: 1015–1021.

Curtis MJ, Bond RA, Spina D, Ahluwalia A, Alexander SPA, Giembycz MA, *et al.* (2015). Experimental design and analysis and their reporting: new guidance for publication in BJP. *Br J Pharmacol* 172: 3461–3471.

Davis AJ, Shi J, Pritchard HA, Chadha PS, Leblanc N, Vasilikostas G, *et al.* (2013). Potent vasorelaxant activity of the TMEM16A inhibitor T16A(inh)-A01. *Br J Pharmacol* 168: 773–784.

Davis JB, Gray J, Gunthorpe MJ, Hatcher JP, Davey PT, Overend P, *et al.* (2000). Vanilloid receptor-1 is essential for inflammatory thermal hyperalgesia. *Nature* 405: 183–187.

Deba F, Bessac BF (2015). Anoctamin-1 Cl<sup>-</sup> channels in nociception: activation by an *N*-aroylaminothiazole and capsaicin and inhibition by T16A[inh]-A01. *Mol Pain* 11: 55.

Gavva NR, Tamir R, Qu Y, Klionsky L, Zhang TJ, Immke D, *et al.* (2005). AMG 9810 [(E)-3-(4-t-butylphenyl)-N-(2,3-dihydrobenzo[b][1,4]dioxin-6-yl)acrylamide], a novel vanilloid receptor 1 (TRPV1) antagonist with antihyperalgesic properties. *J Pharmacol Exp Ther* 313: 474–484.

Huang F, Rock JR, Harfe BD, Cheng T, Huang X, Jan YN, *et al.* (2009). Studies on expression and function of the TMEM16A calcium-activated chloride channel. *Proc Natl Acad Sci U S A* 106: 21 413–21 418.

Imamachi N, Park GH, Lee H, Anderson DJ, Simon MI, Basbaum AI, *et al.* (2009). TRPV1-expressing primary afferents generate behavioral responses to pruritogens via multiple mechanisms. *Proc Natl Acad Sci U S A* 106: 11 330–11 335.

Iqbal J, Tonta MA, Mitsui R, Li Q, Kett M, Li J, *et al.* (2012). Potassium and ANO1/TMEM16A chloride channel profiles distinguish atypical and typical smooth muscle cells from interstitial cells in the mouse renal pelvis. *Br J Pharmacol* 165: 2389–2408.

Jin X, Shah S, Liu Y, Zhang H, Lees M, Fu Z, *et al.* (2013). Activation of the Cl<sup>-</sup> channel ANO1 by localized calcium signals in nociceptive sensory neurons requires coupling with the IP3 receptor. *Sci Signal* 6: ra73.

Kanazawa T, Matsumoto S (2014). Expression of transient receptor potential vanilloid 1 and anoctamin 1 in rat trigeminal ganglion neurons innervating the tongue. *Brain Res Bull* 106: 17–20.

Kilkenny C, Browne W, Cuthill IC, Emerson M, Altman DG (2010). NC3Rs Reporting Guidelines Working Group. *Br J Pharmacol* 160: 1577–1579.

- Lee B, Cho H, Jung J, Yang YD, Yang DJ, Oh U (2014). Anoctamin 1 contributes to inflammatory and nerve-injury induced hypersensitivity. *Mol Pain* 10: 5.
- Liu B, Linley JE, Du X, Zhang X, Ooi L, Zhang H, *et al.* (2010). The acute nociceptive signals induced by bradykinin in rat sensory neurons are mediated by inhibition of M-type K<sup>+</sup> channels and activation of Ca<sup>2+</sup>-activated Cl<sup>-</sup> channels. *J Clin Invest* 120: 1240–1252.
- Lukacs V, Yudin Y, Hammond GR, Sharma E, Fukami K, Rohacs T (2013). Distinctive changes in plasma membrane phosphoinositides underlie differential regulation of TRPV1 in nociceptive neurons. *J Neurosci* 33: 11 451–11 463.
- Luo J, Feng J, Liu S, Walters ET, Hu H (2015). Molecular and cellular mechanisms that initiate pain and itch. *Cell Mol Life Sci* 72: 3201–3223.
- McGrath JC, Lilley E (2015). Implementing guidelines on reporting research using animals (ARRIVE etc.): new requirements for publication in *BJP*. *Br J Pharmacol* 172: 3189–3193.
- Mroz MS, Keely SJ (2012). Epidermal growth factor chronically upregulates Ca<sup>2+</sup>-dependent Cl<sup>-</sup> conductance and TMEM16A expression in intestinal epithelial cells. *J Physiol* 590: 1907–1920.
- Namkung W, Yao Z, Finkbeiner WE, Verkman AS (2011). Small-molecule activators of TMEM16A, a calcium-activated chloride channel, stimulate epithelial chloride secretion and intestinal contraction. *FASEB J* 25: 4048–4062.
- Pawson AJ, Sharman JL, Benson HE, Faccenda E, Alexander SP, Buneman OP *et al.*, NC-IUPHAR (2014). The IUPHAR/BPS guide to PHARMACOLOGY: an expert-driven knowledge base of drug targets and their ligands. *Nucleic Acids Res* 42: D1098–D1106.
- Pineda-Farias JB, Barragán-Iglesias P, Loeza-Alcocer E, Torres-López JE, Rocha-González HI, Pérez-Severiano F, *et al.* (2015). Role of anoctamin-1 and bestrophin-1 in spinal nerve ligation-induced neuropathic pain in rats. *Mol Pain* 11: 41.
- Ro JY, Lee JS, Zhang Y (2009). Activation of TRPV1 and TRPA1 leads to muscle nociception and mechanical hyperalgesia. *Pain* 144: 270–277.
- Ross RA (2003). Anandamide and vanilloid TRPV1 receptors. *Br J Pharmacol* 140: 790–801.
- Sala-Rabanal M, Yurtsever Z, Nichols CG, Brett TJ (2015). Secreted CLCA1 modulates TMEM16A to activate Ca<sup>2+</sup>-dependent chloride currents in human cells. *Elife* 4: e05875.
- Schroeder BC, Cheng T, Jan YN, Jan IY (2008). Expression cloning of TMEM16A as a calcium-activated chloride channel subunit. *Cell* 134: 1019–1029.
- Singh RD, Gibbons SJ, Saravanaperumal SA, Du P, Hennig GW, Eisenman ST, *et al.* (2014). Ano1, a Ca<sup>2+</sup>-activated Cl<sup>-</sup> channel, coordinates contractility in mouse intestine by Ca<sup>2+</sup> transient coordination between interstitial cells of Cajal. *J Physiol* 592: 4051–4068.
- Sun M, Sui Y, Li L, Su W, Hao F, Zhu Q, *et al.* (2014). Anoctamin 1 calcium-activated chloride channel downregulates estrogen production in mouse ovarian granulosa cells. *Endocrinology* 155: 2787–2796.
- Sun YG, Chen ZF (2007). A gastrin-releasing peptide receptor mediates the itch sensation in the spinal cord. *Nature* 448: 700–703.
- Sun YG, Zhao ZQ, Meng XL, Yin J, Liu XY, Chen ZF (2009). Cellular basis of itch sensation. *Science* 325: 1531–1534.
- Takayama Y, Shibasaki K, Suzuki Y, Yamanaka A, Tominaga M (2014). Modulation of water efflux through functional interaction between TRPV4 and TMEM16A/anoctamin 1. *FASEB J* 28: 2238–2248.
- Takayama Y, Uta D, Furue H, Tominaga M (2015). Pain-enhancing mechanism through interaction between TRPV1 and anoctamin 1 in sensory neurons. *Proc Natl Acad Sci USA* 112: 5213–5218.
- Tominaga M, Caterina MJ, Malmberg AB, Rosen TA, Gilbert H, Skinner K, *et al.* (1998). The cloned capsaicin receptor integrates multiple pain-producing stimuli. *Neuron* 21: 531–543.
- Watanabe H, Vriens J, Prenen J, Droogmans G, Voets T, Nilius B (2003). Anandamide and arachidonic acid use epoxyeicosatrienoic acids to activate TRPV4 channels. *Nature* 424: 434–438.
- Willis EF, Clough GF, Church MK (2004). Investigation into the mechanisms by which nedocromil sodium, frusemide and bumetanide inhibit the histamine-induced itch and flare response in human skin *in vivo*. *Clin Exp Allergy* 34: 450–455.
- Woodbury CJ, Zwick M, Wang S, Lawson JJ, Caterina MJ, Koltzenburg M, *et al.* (2004). Nociceptors lacking TRPV1 and TRPV2 have normal heat responses. *J Neurosci* 24: 6410–6415.
- Xu H, Blair NT, Clapham DE (2005). Camphor activates and strongly desensitizes the transient receptor potential vanilloid subtype 1 channel in a vanilloid-independent mechanism. *J Neurosci* 25: 8924–8937.
- Yang YD, Cho H, Koo JY, Tak MH, Cho Y, Shim WS, *et al.* (2008). TMEM16A confers receptor-activated calcium-dependent chloride conductance. *Nature* 455: 1210–1215.
- Yin S, Luo J, Qian A, Du J, Yang Q, Zhou S, *et al.* (2013). Retinoids activate the irritant receptor TRPV1 and produce sensory hypersensitivity. *J Clin Invest* 123: 3941–3951.
- Yin S, Luo J, Qian A, Yu W, Hu H (2014). LE135, a retinoid acid receptor antagonist, produces pain through direct activation of TRP channels. *Br J Pharmacol* 171: 1510–1520.
- Zhang XD, Lee JH, Lv P, Chen WC, Kim HJ, Wei D, *et al.* (2015). Etiology of distinct membrane excitability in pre- and posthearing auditory neurons relies on activity of Cl<sup>-</sup> channel TMEM16A. *Proc Natl Acad Sci U S A* 112: 2575–2580.

## Supporting Information

Additional Supporting Information may be found in the online version of this article at the publisher's web-site:

<http://dx.doi.org/10.1111/bph.13420>

**Figure S1** Pharmacological blockade of TMEM16A function attenuated Eact-induced itch- and pain-related behaviors. (A) Co-application of T16Ainh-A01 (A01, 10 μg) suppressed the scratching response elicited by intradermal injection of 50 μl Eact (4.67 mM) into the rostral back. Please note that 10 μg is the highest dose for A01 used *in vivo* (Pineda-Farias *et al.*, 2015). (B) Co-application of T16Ainh-A01 (A01, 10 μg) suppressed the flinching and licking behaviors produced by intraplantar injection of 20 μl of Eact (4.67 mM). (C) Time course of thermal hypersensitivity in animals treated with Eact (intraplantar, 20 μl, 4.67 mM). Co-applied A01 (0.48 M) attenuated Eact-induced decrease of paw withdrawal latency. \**p*<0.05, \*\**p*<0.01, \*\*\**p*<0.001 Eact group versus vehicle group; +*p*<0.05, ++*p*<0.01 Eact group versus Eact + A01 group; #*p*<0.05, ##*p*<0.01 Eact + A01 group versus A01 group; *n* = 7–8 mice per group. A01 = T16Ainh-A01.

**Figure S2** TMEM16A increases capsaicin response when co-expressed with mTRPV1 in HEK293T cells. (A) and (B) Representative traces show that capsaicin (0.3 μM) activated an

outward current at +60 mV and an inward current at -60 mV in HEK293T cells expressing mTRPV1 alone (A) or co-expressing mTRPV1 and mTMEM16A (B). (C) Comparison of the peak capsaicin current densities between cells expressing mTRPV1 alone and cells co-expressing mTRPV1 and mTMEM16A (\* $p < 0.05$ ,  $n = 7-8$  cells per group).

**Figure S3** siRNA knockdown of TMEM16A did not affect Eact-activated membrane currents in mTRPV1-expressing HEK293T cells. (A) Immunoblotting results show that transfection with small interfering RNA (siRNA, 200 nM) against TMEM16A, but not scrambled siRNA control (Scr. siRNA, 200 nM), markedly reduced TMEM16A protein expression in the mTRPV1-expressing HEK293T cells. \*\*\* $p < 0.001$ ;  $n = 3$  per group. (B) Representative Eact (10  $\mu\text{M}$ )-activated current traces in response to voltage ramp from -100 mV to +100 mV in mTRPV1-expressing HEK293T cell transfected with either scrambled siRNA control or siRNA against TMEM16A. (C) Quantification of Eact (10  $\mu\text{M}$ )-activated current responses in mTRPV1-expressing HEK293T transfected with scrambled siRNA control or siRNA against TMEM16A. Cells were voltage-clamped at -60 mV (NS: no significant difference,  $n = 6$  per group).

**Figure S4** The TRPV1 inhibitor capsazepine nearly abolished Eact-activated membrane currents in cultured DRG neurons. (A) Representative current traces show that Eact (100  $\mu\text{M}$ ) activated an outward current at +60 mV and an inward current at -60 mV in a wt DRG neuron. The whole-cell currents evoked by Eact were substantially suppressed by capsazepine (10  $\mu\text{M}$ ). The inhibitory effect of

capsazepine was partially reversible after washout. (B) Current-voltage relationship of Eact-activated currents taken at the time points specified in A. (C) Quantification of averaged Eact-activated currents with and without capsazepine in DRG neurons voltage-clamped at -60 mV. \*\*\* $P < 0.001$ , NS: no significant difference,  $n = 10$ .

**Figure S5** A01, the selective inhibitor of TMEM16A, did not inhibit Eact-activated membrane currents in DRG neurons. (A) Representative current traces show that Eact (100  $\mu\text{M}$ ) activated an outward current at +60 mV and an inward current at -60 mV in a wild type DRG neuron. The whole-cell currents evoked by Eact were slightly suppressed by A01 (10  $\mu\text{M}$ ). (B) Current-voltage relationship of Eact-activated current taken at the time points specified in A. (C) Quantification of Eact current densities in DRG neurons voltage-clamped at -60 mV. There was no significant difference among Eact responses ( $n = 9$ ). NS: no significant difference, A01 = T16Ainh-A01.

**Figure S6** Eact-activated membrane currents in cultured sensory neurons are not  $\text{Cl}^-$  currents. (A) Representative current traces show that Eact (100  $\mu\text{M}$ ) activated an outward current at +60 mV and an inward current at -60 mV in a wt DRG neuron recorded with a  $\text{Cl}^-$ -free pipette solution. (B) Current-voltage relationship of Eact-activated currents taken at the time points specified in A. (C) Comparison of the peak Eact-activated current densities in DRG neurons with 140 mM  $\text{Cl}^-$  (High  $[\text{Cl}^-]_i$ ) pipette solution and 0 mM  $\text{Cl}^-$  (Free  $[\text{Cl}^-]_i$ ) pipette solution voltage-clamped at -60 mV (NS: no significant difference,  $n = 9-10$  per group).